210 (1972), and 29, 55 (1972).
[3]J. Nation, Appl. Phys. Lett. 17, 991 (1970).
[4]M. Friedman, Phys. Rev. Lett. 31, 1107 (1973).
[5]M. Friedman, Appl. Phys. Lett. 26, 366 (1975).
[6]Y. Carmel and J. Nation, Phys. Rev. Lett. 31, 286 (1973).
[7]M. Friedman and M. Ury, Rev. Sci. Instrum. 41, 1334 (1970).
[8]The damage on the witness plate was produced by a single shot. The material blowout (the white portion) gives the time average of the beam dimensions (e.g., position and thickness). In the experiment the witness plate covered the whole cross section of the drift tube.
[9]M. Friedman and D. Hammer, Appl. Phys. Lett. 21, 174 (1972).
[10]M. Friedman, Appl. Phys. Lett. 24, 303 (1974).
[11]C. A. Kapetanakos and A. W. Trivelpiece, J. Appl. Phys. 42, 4841 (1971).
[12]V. L. Granatstein, M. Herndon, R. K. Parker, and P. Sprangle, IEEE J. Quantum Electron. 10, 651 (1974).
[13]N. Kovalev *et al.*, Pis'ma Zh. Eksp. Teor. Fiz. 18, 232 (1973) [JETP Lett. 18, 138 (1973)]; Y. Carmel, J. Ivers, R. E. Kribel, and J. Nation, Phys. Rev. Lett. 33, 1273 (1974).

Self-Ducting of Large-Amplitude Whistler Waves*

R. L. Stenzel
TRW Systems, Redondo Beach, California 90278
(Received 12 May 1975)

Whistler waves are launched from an electric dipole of length L in a large-volume laboratory plasma. With increasing wave amplitude the radiation pattern narrows and finally forms a duct of diameter $d \simeq L \simeq \lambda_{||}$. The ducted waves propagate nearly undamped. The observed nonlinear effects are explained by wave-particle interactions.

Currently much attention has been given to the problems of exciting large-amplitude whistler waves from spacecrafts with long wire antennas. The linear wave properties[1] and the behavior of antennas at small amplitudes[2] seem well understood; however, at large amplitudes nonlinear sheath effects, modifications of the plasma by the large-amplitude wave, and parametric instabilities make a theoretical prediction of the radiation problem very difficult and call for actual experiments. The advantages of scaled laboratory experiments over field experiments in terms of cost, control of parameters, reproducibility, and variety of diagnostics are obvious but were previously outweighed by the disadvantage of boundary effects in most small-scale laboratory plasmas. I have therefore constructed an unusually large (diameter $\sim 10\lambda_{||}$, length $\sim 100\lambda_{||}$), quiescent, collisionless, magnetized-plasma device and investigated the dipole-radiation problem at both small and large amplitudes. I observe that with increasing wave amplitude the dipole-antenna radiation pattern narrows and eventually collapses into a narrow well-collimated duct in which the wave propagates virtually undamped. In the duct the electron distribution function is found to be modified and the density is slightly reduced. The observed instability is qualitatively explained by wave-particle interactions[3] rather than ducting along field-aligned density perturbations.[1]

The experiment is performed in a discharge plasma produced in krypton with an indirectly heated, oxide-coated cathode of diameter $d = 50$ cm. The plasma column is substantially uniform over 40 cm in diameter (see Fig. 1) and 300 cm in length, has a peak density $n_e \simeq 10^{12}$ cm^{-3}, electron temperature $T_e \simeq 2$ eV, degree of ionization $n_e/n_n \simeq 10\%$, collision rate $\nu_{en}/\omega \lesssim 10^{-3}$, and is uniformly ($\pm 0.5\%$) magnetized with $B_0 \simeq 100$ G. The discharge is pulsed on for approximately 3 msec with repetition time of 500 msec [see Fig. 2(a)]. Whistler waves of frequency $\omega/2\pi \simeq 150$ MHz are excited with a linear balanced electric dipole (4.4

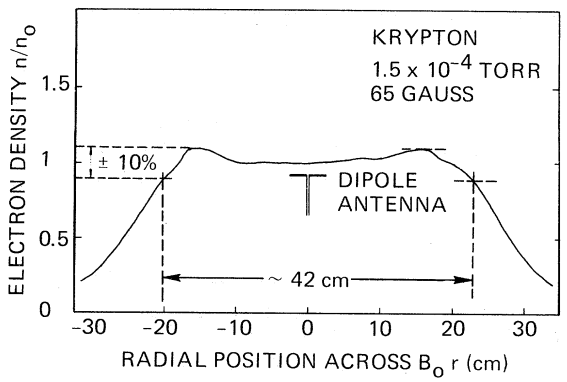

FIG. 1. Normalized radial density profile with antenna size and location as indicated.

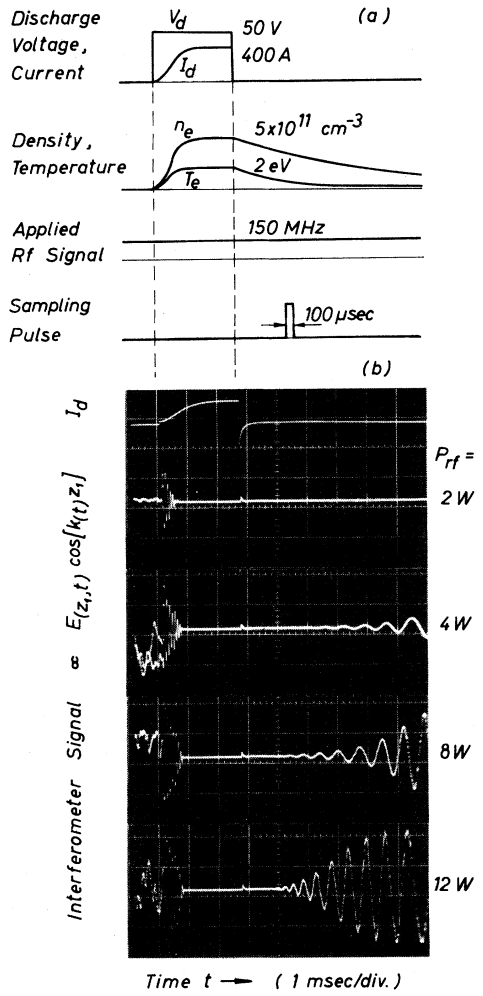

FIG. 2. (a) Typical time sequence of the pulsed plasma and sampled interferometer measurements. (b) Interferometer signal versus time at different rf power levels applied to the exciter dipole. Axial distance z_1 = 95 cm, $\omega/\omega_c = 0.85$.

cm length) movable in the axial direction (parallel to $\vec{B}_0$) and detected with a short (1 cm) coax-fed wire antenna movable in the radial direction. The rf signal is applied in steady state for power levels $P \lesssim 10$ W and in pulsed mode for $P \lesssim 80$ W. The received signal is amplified and applied to an interferometer circuit whose output, $V_{\text{out}} \propto E(z)\cos(kz)$, is sampled at a desired time during or after the discharge and then averaged over many events. Plasma diagnostics include Langmuir probes and a 70-GHz interferometer.

I have first verified the small-amplitude propagation characteristics. The dispersion relation for the right-hand circularly polarized waves propagating along B_0 is given by

$$k_{\parallel}{}^2c^2/\omega^2 = 1 + \omega_p{}^2/(\omega k v_e)Z_+(\zeta_e), \quad (1)$$

where $\zeta_e = (\omega - \omega_c)/(k_{\parallel} v_e)$ and Z_+ is the plasma dispersion function.[4] For $|\zeta_e| \gtrsim 3$, the cold-plasma approximation $k_{\parallel}{}^2c^2/\omega^2 \simeq 1 - \omega_p{}^2/(\omega^2 - \omega\omega_c)$ is valid. In the parameter range $10 < \omega_p/\omega < 25$ and $\omega/\omega_c < 0.75$ there is good agreement with the approximation while for $\omega/\omega_c > 0.75$ thermal corrections, according to Eq. (1), become noticeable.

The observed wave damping arises from several contributions. (a) Geometric effects: The dipole launches spherical rather than plane waves; (b) non-Maxwellian electron distribution functions: The presence of energetic electrons [bump-on-tail distribution in $f_e(v_{\parallel})$] during the discharge yields lower damping than in the afterglow where $f_e(\vec{v})$ is approximately Maxwellian; (c) collisions: $\nu_{en}/\omega \sim 10^{-3}$, $\nu_{ei}/\omega \sim 10^{-2}$; (d) cyclotron damping dominates as $\omega/\omega_c \to 1$.

The polarization of the wave is determined by rotating the linear exciter dipole around the axis (parallel to $\vec{B}_0$) and translating it along $\vec{B}_0$ so as to maintain a constant phase at the receiver antenna. The polarization rotates in the same sense as electrons rotate around $\vec{B}_0$. The received amplitude is observed to be independent of dipole rotation; thus the wave is right-hand circularly polarized.

The large-amplitude effects are apparent in Fig. 2(b) which shows a set of interferometer traces versus time at different power levels applied to the antenna. The probe separation is fixed at approximately $z = 95$ cm, and a constant rf signal is applied in steady state. The oscillations in the interferometer signal, $E(z)\cos(k_{\parallel} z)$, are due to the increase and decrease of $k_{\parallel}$ with density in the pulsed plasma. The oscillation period has no relation to the whistler-wave period but the oscillation amplitude is directly proportional to the received-wave amplitude. At small power levels a number of fringes are seen in the beginning of the discharge where a relatively high population of fast electrons is present ($v_{\parallel} \simeq 4\times10^8$ cm/sec $\gg v_{\perp}$). Later the damping is too high to observe the wave with the same sensitivity. However, with increasing power level the waves begin to appear in the afterglow and furthermore, their amplitudes grow in time. Growth rate and saturation amplitude increase with applied power.

The large-amplitude whistler wave gives rise to a nonlinear spatial behavior as indicated in

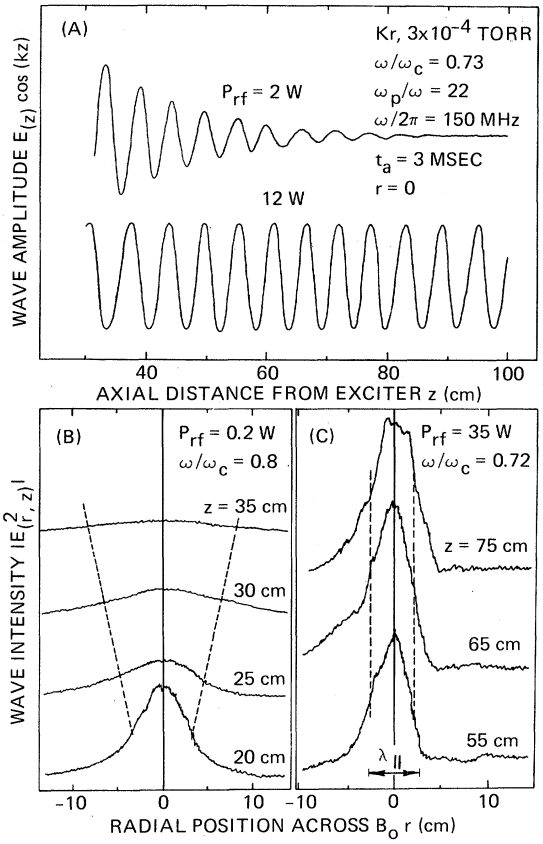

FIG. 3. (a) Interferometer trace versus axial position at small applied rf power levels (top trace) and large levels (bottom trace, reduced gain), sampled at afterglow time t_a. (b) Radial-wave intensity profiles at small power levels showing divergent radiation pattern. Note the absence of resonance cones due to finite dipole length ($L \simeq \lambda_{||}$). (c) Wave intensity versus r at distances z from exciter antenna driven at large rf power levels. The wave has created a field-aligned duct in which it propagates undamped. Afterglow time t_a = 3 msec.

Fig. 3(a) which shows axial interferometer traces at t_a = 3 msec in the afterglow for small (top trace) and high (bottom trace, reduced gain) power levels. With increasing power level the spatial damping is reduced until the wave propagates almost undamped. Only near the antenna the amplitude decays superimposed with a damped oscillatory pattern at high powers. Figure 3(b) shows the wave intensity $|E^2|$ versus radial ($\perp \vec{B}_0$) position at different axial ($|| \vec{B}_0$) distances from the exciter at a small power level and Fig. 3(c) similarly at a high power level. At small amplitudes the radiation diverges from the dipole which accounts for most of the observed amplitude decay with distance. However, at high power levels

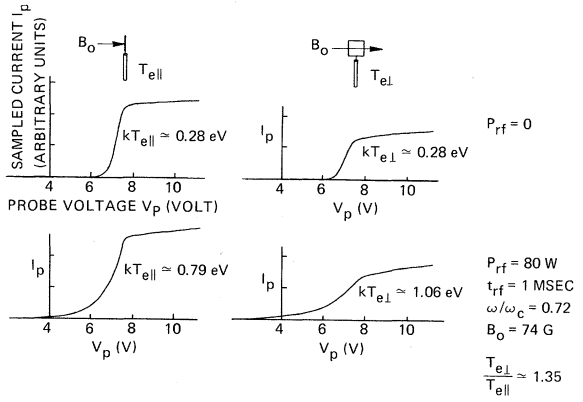

FIG. 4. Sampled Langmuir-probe traces at afterglow time t_a = 3 msec in the absence (top traces) and presence (bottom traces) of a large-amplitude whistler-wave burst. Probe location $r = 0$, $z = 50$ cm.

the wave energy is confined to a narrow region of diameter $d \sim 5$ cm which does not broaden with increasing distance up to $20\lambda_{||} \simeq 100$ cm along $\vec{B}_0$. Thus, the large-amplitude wave has created a field-aligned duct in which it is guided. The guided waves are plane waves as determined from phase measurements across the duct ($\varphi(r) = kz$ = const). Once the duct has been created one can also guide small-amplitude whistler waves at other frequencies in it. After the end of the large-amplitude whistler wave pulse the duct decays within approximately 500 μsec. The build-up time depends on power level and is approximately 500 μsec at P_{max} = 80 W.

Evidently, the duct is formed by changing some basic plasma parameters. I have therefore performed sampled Langmuir-probe measurements in the duct region during and after the perturbing rf pulse. Figure 4 shows Langmuir-probe traces at 3 msec in the afterglow with and without the large-amplitude whistler waves. A plane thin Langmuir probe (4 mm×4 mm×0.2 mm) is used, once aligned with its surface normal parallel to $\vec{B}_0$ so as to measure $T_{e||}$ and then rotated by 90° so as to collect mainly electrons across $\vec{B}_0$ (electron Larmor radius $r_{ce} \simeq 0.5$ mm > probe thickness). In the absence of the whistler wave $T_{e||} \simeq T_{e\perp} \simeq 0.28$ eV but after a 1-msec rf burst (80-W applied power) the electrons are heated ($T_{e||} \simeq 0.79$ eV, $T_{e\perp} \simeq 1.06$ eV), a temperature anisotropy has developed, $f_e(\vec{v})$ deviates from a Maxwellian due to an energetic tail, and the electron density has decreased. These modifications occur only in the duct region. By sampling the probe characteristics after the end of the rf burst and observ-

ing the perturbation relax it has been verified that the results are not caused by rf rectification on the probe sheath.

The above described experimental observations may support the following qualitative physical picture of the nonlinear interactions: The large rf field in the vicinity of the antenna generates fast electrons by transit-time and collisional effects. Since tails up to 15 eV are directly observable it is possible that a small fraction ($<10^{-3}$) of fast electrons is present which resonate with the wave $[(\omega_c - \omega)/k_{||} = v_{||} \simeq 3 \times 10^7$ cm/sec in Fig. 3; $\frac{1}{2} m v_{||}^2 = 27$ eV]. Trapped-particle effects[3] would give rise to a periodic amplitude behavior near the exciter with subsequent rapid phase mixing and formation of a constant-amplitude pattern consistent with the observation.

As the trapped particles are confined along $\vec{B}_0$ the nonlinear effects are field aligned and the resulting constant-amplitude pattern is reminiscent of whistler-wave ducting. The present nonlinear ducting mechanism due to wave-particle interactions is however different from the familiar ionospheric ducting[1] involving wave refraction in gentle field-aligned density perturbations. Although as a result of the temperature increase in the nonlinear ducts a density depression ($\delta n/n \gtrsim 10\%$) is also present, it is not believed to contribute significantly to the ducting process for two reasons: First, the ducts can be very narrow (diameter $\lesssim \lambda_{||}/2$) without observing cutoff effects; second, by producing similar density depressions with obstacles in the plasma no ducting is seen.

The observed temperature anisotropy also contributes to a decrease in wave damping but is not sufficiently high for marginal stability[5] $[(T_{e\perp}/T_{e||})_{\gamma=0} = (1 - \omega/\omega_c)^{-1} \simeq 3.7]$.

It should be pointed out that the ducted whistler waves have longitudinal field components. This fact complicates the comparison with available theories on large-amplitude whistlers which to my knowledge only consider transverse modes.

The author gratefully acknowledges most fruitful discussions with R. W. Fredricks, F. Coroniti, D. Arnush, K. Nishikawa, and the technical assistance by W. Dabbs and W. Daley.

*Work supported by TRW IR&D funds and National Aeronautics and Space Administration Contract No. NASA-31175.

[1]R. A. Helliwell, *Whistlers and Related Ionospheric Phenomena* (Stanford Univ. Press, Stanford, Calif., 1965).

[2]J. R. Wait, *Electromagnetics and Plasmas* (Holt, Rinehart and Winston, New York, 1968); J. O. Thomas and B. J. Landmark, *Plasma Waves in Space and in the Laboratory* (American Elsevier, New York, 1969).

[3]R. F. Lutomirski and R. N. Sudan, Phys. Rev. 147, 156 (1966); P. Palmadesso and G. Schmidt, Phys. Fluids 14, 1411 (1971), and 15, 485 (1972); S. L. Ossakow, E. Ott, and I. Haber, Phys. Fluids 15, 2314 (1972).

[4]B. D. Fried and S. D. Conte, *The Plasma Dispersion Function* (Academic, New York, 1961).

[5]S. L. Ossakow, E. Ott, and I. Haber, Phys. Fluids 15, 2314 (1972); R. C. Davidson, D. A. Hammer, I. Haber, and C. E. Wagner, Phys. Fluids 15, 317 (1972).

Properties of Nonneutral Plasma*

J. H. Malmberg and J. S. deGrassie
Department of Physics, University of California, San Diego, La Jolla, California 92037
(Received 24 February 1975)

We describe an apparatus for producing a magnetized column of nonneutral electron plasma which is many Debye lengths in radius. The plasma exhibits the linear and nonlinear electron-wave effects observed in neutralized plasmas.

In recent years increasing research has been devoted to the equilibrium and stability properties of plasmas for which all particles have the same sign of electric charge.[1,2] It is known theoretically that such nonneutral plasmas exhibit shielding on the scale of their Debye length[3] and collective effects like plasma waves.[4] We here describe an apparatus which generates a magnetized column of electron gas which is a nonneutral plasma by the criterion that the Debye length is small compared to the radius of the column. We also report experimental verification of the properties of waves in this plasma. Except for a slow rotation, the plasma is at rest in the laboratory frame of reference. This fact distinguishes the present plasma from that obtained in electron-

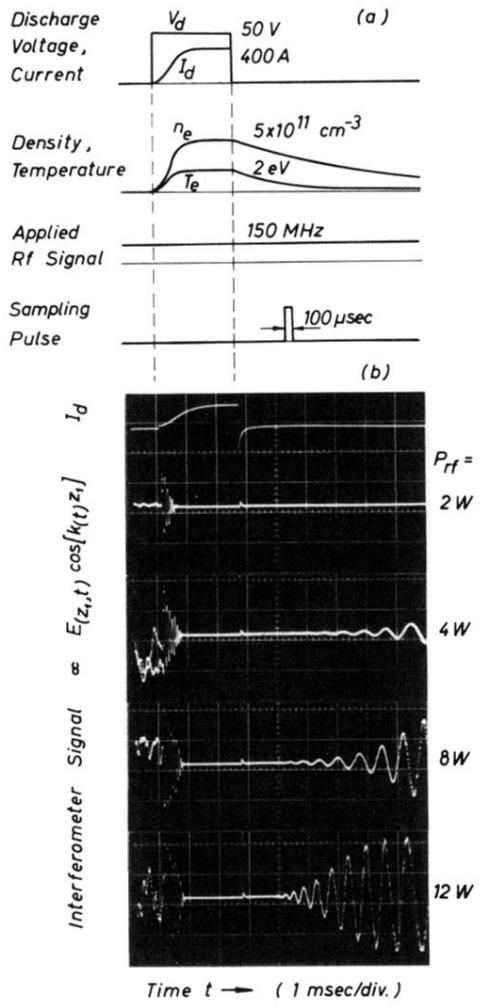

FIG. 2. (a) Typical time sequence of the pulsed plasma and sampled interferometer measurements. (b) Interferometer signal versus time at different rf power levels applied to the exciter dipole. Axial distance z_1 = 95 cm, $\omega/\omega_c = 0.85$.